Séminaire Poincaré 1 (2003) 21 – 37 **Séminaire Poincaré**

Condensed Matter Approaches to Quantum Gases

G.V. Shlyapnikov

1 Introduction

The discovery of Bose-Einstein condensation (BEC) in dilute atomic gases of Rb [1], Na [2], and Li [3] in magnetic traps has stimulated an enormous revival of the interest in macroscopic quantum behavior of dilute gases at low temperature. Up to this discovery the main emphasis had been on the development of efficient evaporative [4] and optical cooling [5] methods to reach the critical temperature $T_c \lesssim 1$ μK and density $n \sim 10^{14}$ cm^{-3} for the observation of BEC. Experiments with trapped Bose-condensed gases have revealed profound condensed matter behavior of these extremely dilute systyms. The goal of this lecture is to describe the key features of this behavior and discuss theoretical approaches that are being used in the field of quantum gases.

The condensed matter behavior of quantum Bose gases originates from the dominant role of interparticle interactions once a single quantum state becomes macroscopically occupied [6]. So was the difference in free expansion between condensate and thermal gas clouds after switching off the trap, important supporting evidence for the presence of a Bose-condensed state. Differences from the non-degenerate behavior were strongly pronounced in studies of eigenfrequencies and temperature-dependent damping of the lowest excitations. The most profound features of the macroscopic quantum nature of dilute Bose-condensed gases were found in the MIT experiment on interference of two independently prepared condensates [7], and in the JILA experiment [8] on a strong reduction of 3-body recombination due to a change of local correlation properties in the presence of a condensate. In a later stage, superfluid character of Bose-condensed gases was demonstrated in experiments on creating vortex [9] and soliton [10] structures, in the studies of scissors excitation modes [11], and in the measurement of the critical velocity for superfluidity [12].

Theoretical and numerical studies of trapped Bose-condensed gases were first focused on the ground-state properties and elementary excitations of a static gas or on coherently evolving condensates in the mean-field approach. Studies beyond the mean-field succeeded in describing temperature-dependent damping rates and frequency shifts of low-energy excitations of a trapped condensate [6, 13, 14]. These studies were followed by and done in parallel with investigations of the zero- and finite-temperature dynamics of vortices [9] and solitons [10, 15]. Theoretical developments in the field of trapped Bose-condensed gases have become successful due to a wide use of condensed matter approaches, such as the Gross-Pitaevskii equation for a trapped condensate, Bogoliubov equations for the excitations, finite-temperature perturbation theory, etc. The presence of the trapping potential and a finite size of the system required a serious reformulation of these approaches. Investigations of a sharp cross-over to the BEC regime [16] revived an interest in the general question of how the transition temperature depends on the interaction between particles and stimulated theoretical and Monte Carlo studies in this direction. On the basis of both experiment and theory, equilibrium properties and dynamics of trapped Bose-condensed gases are now rather well understood.

In the last years a lot of attention has been focused on phase coherence phenomena. These studies are expected to provide new fundamental insights into the nature of macroscopic quantum states and are important for future applications, such as the creation atom lasers - devices for generation of coherent matter waves. Recent theoretical studies [17] have revealed that in elongated 3D traps the finite-temperature equilibrium state can be a *quasicondensate* characterized by suppressed density fluctuations and axially fluctuating phase. The existence of these phase-fluctuating BEC states has been found in Hannover [18] and Orsay [19] experiments. In the present stage, the phenomenon of quasicondensation is one of the important issues in the studies of quantum gases.

2 Scaling approach

Time-dependent variations of the trapping potential lead to the evolution of a trapped condensate. This evolution is quite different from that of a classical gas under the same conditions. The simplest example is a free expansion of the gas after abruptly switching off the trap as in the first JILA [1] and MIT [2] experiments. In this lecture we discuss the scaling approach [20, 21, 22] for describing the evolution of a condensate with a fixed number of particles in a harmonic potential

$$V(\mathbf{r}) = \sum_i m\omega_i^2 r_i^2/2 \tag{1}$$

under time-dependent variations of the frequencies $\omega_i(t)$. An initially static condensate is assumed to be in equilibrium in an external potential $V(\mathbf{r})$ with constant frequencies $\omega_{0i} = \omega_i(0)$.

We assume that the mean interparticle separation greatly exceeds the radius of interaction between them and $n|a|^3 \ll 1$, where a is the scattering length. Therefore one can use a contact potential of pair interaction characterized by a single parameter, the scattering length a. Then the Hamiltonian of the system takes the form

$$\hat{H} = \int d\mathbf{r}\, \hat{\psi}^\dagger \{-(\hbar^2/2m)\Delta + V(\mathbf{r}) + (g/2)\hat{\psi}^\dagger\hat{\psi}\}\hat{\psi}, \tag{2}$$

and the Schrödinger equation for the Heisenberg field operator of atoms, $\hat{\psi}(\mathbf{r}, t)$, reads

$$i\hbar(\partial\hat{\psi}/\partial t) = -(\hbar^2/2m)\Delta\hat{\psi} + V(\mathbf{r})\hat{\psi} + g\hat{\psi}^\dagger\hat{\psi}\hat{\psi}, \tag{3}$$

where the last term in the right-hand side of Eq.(3) describes the interaction between particles, and the coupling constant is $g = 4\pi\hbar^2 a/m$. The field operator $\hat{\psi}$ can be represented as a sum of the non-condensed part $\hat{\psi}'$ and the condensate wave function ψ_0 which is a c-number (see, e.g., [23]):

$$\hat{\psi} = \psi_0 + \hat{\psi}'. \tag{4}$$

Averaging both sides of Eq.(3) and omitting contributions originating from the non-condensed part $\hat{\psi}'$, we obtain the familiar mean-field Gross-Pitaevskii equation:

$$i\hbar(\partial\psi_0/\partial t) = -(\hbar^2/2m)\Delta\psi_0 + V(\mathbf{r})\psi_0 + g|\psi_0|^2\psi_0. \tag{5}$$

The condensate wave function is normalized by the condition

$$\int d\mathbf{r}|\,\psi_0|^2 = N_0, \tag{6}$$

where N_0 is the number of particles in the condensate.

In equilibrium the time dependence of the condensate wave function is reduced to $\psi_0 \propto \exp(-i\mu t)$, where μ is the chemical potential. Then Eq.(5) takes a stationary form describing the initial static condensate:

$$-(\hbar^2/2m)\Delta\psi_0 + V(\mathbf{r})\psi_0 + g|\psi_0|^2\psi_0 - \mu\psi_0 = 0. \tag{7}$$

From this point on we consider a repulsive interaction between particles ($a > 0$). The shape of ψ_0 is determined by a balance between the interparticle repulsion and the confining potential. In the so-called Thomas-Fermi regime the mean-field interaction greatly exceeds the spacing between the trap levels, and the kinetic energy term in Eq.(7) is not important. One then has the well-known algebraic solution for the condensate wave function [24, 25]:

$$\psi_0 = \sqrt{(\mu - V(\mathbf{r})/g}\exp(-i\mu t). \tag{8}$$

This solution is valid in the spatial region where the argument of the square root is positive, and $\psi_0 = 0$ otherwise. The chemical potential is given by $\mu = n_0 g$, with n_0 being the maximum

condensate density. In a harmonic confining potential the condensate density $|\psi_0|^2$ has a shape of an inverted parabola, with the size in the i-th direction $R_{0i} = (2\mu/m\omega_{0i}^2)^{1/2}$.

For analyzing the evolution of the condensate wave function under time-dependent variations of the frequencies ω_i at $t \geq 0$, we return to Eq.(5) and introduce scaling parameters $b_i(t)$. Turning to rescaled coordinates $\rho_i = r_i/b_i(t)$ we search for the solution of Eq.(5) in the form

$$\psi_0(\mathbf{r}, t) = \mathcal{V}^{-1/2}(t)\chi_0(\rho_i, \tau(t)) \exp\left(i\Phi(\mathbf{r}, t)\right), \tag{9}$$

where the dimensionless volume is $\mathcal{V}(t) \prod_i b_i(t)$, and the rescaled time $\tau(t) = \int^t dt'/\mathcal{V}(t')$. Substituting Eq.(9) into Eq.(5) we require the cancellation of $\nabla_\rho \chi_0$ terms, which gives the phase

$$\Phi(\mathbf{r}, t) = (m/2\hbar) \sum_i r_i^2 [\dot{b}(t)/b(t)]. \tag{10}$$

Then, for the scaling parameters governed by equations

$$\ddot{b}_i + \omega_i^2(t) b_i = \omega_{i0}^2/b_i \mathcal{V}(t), \tag{11}$$

with initial conditions $b_i(0) = 1$, $\dot{b}_i(t) = 0$, we arrive at the equation of motion

$$i\hbar(\partial\chi_0/\partial t) = K[\chi_0] + (m/2) \sum_i \omega_{0i}^2 \rho_i^2 \chi_0 + g|\chi_0|^2 \chi_0, \tag{12}$$

where the kinetic energy term is given by

$$K[\chi_0] = -\frac{\hbar^2}{2m} \sum_i \frac{\mathcal{V}(t)}{b_i^2(t)} \frac{\partial^2 \chi_0}{\partial \rho_i^2}. \tag{13}$$

In the Thomas-Fermi regime the ratio of the kinetic energy term to the non-linear interaction term in Eq.(12) is initially very small and scales as $\eta(t) = \sum_i [\hbar\omega_{0i}/\mu b_i(t)]^2 \mathcal{V}(t)$. The condition $\eta(t) \ll 1$ is satisfied on a long (or even infinite) time scale. Then the kinetic energy term can be omitted and in rescaled variables ρ, τ the equation of motion is reduced to an equation for the initial static Thomas-Fermi condensate. The latter equation is nothing else than Eq.(7) in which the kinetic energy term is neglected. The solution is given by Eq.(8), with $V(\mathbf{r})$ (1). Thus, Eqs. (9) and (12) give a universal scaling solution for $\psi_0(\mathbf{r}, t)$ under arbitrary variations of the frequencies and anisotropy of the external potential:

$$\chi_0(\rho_i, \tau(t)) = \frac{1}{g} \left(\mu - \frac{m}{2} \sum_i \frac{\omega_{0i}^2 r_i^2}{b_i^2(t)} \right)^{1/2} \exp\left[-i\mu\tau(t)\right]. \tag{14}$$

The condensate preserves its shape, and at time t the ratio of the condensate size in the i-th direction, $R_i(t)$, to the initial size R_{0i} is given by the value of the scaling parameter $b_i(t)$.

In symmetrical two-dimensional traps, or in infinitely long cylindrical traps, the scaling solution (9) is exact [20, 22]. In these cases the scaling parameters $b_x^2(t) = b_y^2(t) = \mathcal{V}(t)$, and the kinetic energy term in equation of motion (12) becomes $K[\chi_0] = -(\hbar^2/2m)\Delta_\rho \chi_0$. Accordingly, in rescaled variables this equation is the same as Eq.(7) for the initial static condensate, irrespective of the shape of the condensate wave function. Thus, any initial shape governed by Eq.(7) is preserved and the condensate size is rescaled as $b(t)$.

Interestingly, the evolution dynamics of the quantum coherent state (condensate) is governed by *classical* equations of motion (11). These equations follow from the *classical* Hamiltonian of "scaling dynamics" [20]

$$H_{sd} = \frac{1}{2} \sum_i (p_i^2 + \omega_i^2(t) q_i^2) + \frac{\bar{\omega}_0^2}{\prod_i q_i}, \tag{15}$$

where $\bar{\omega}_0$ is the geometrical mean of the initial trap frequencies, $q_i = (\bar{\omega}_0/\omega_{0i}) b_i$, $p_i = \dot{q}_i$, and $\prod_i q_i = \mathcal{V}$. The Hamiltonian H_{sd} describes harmonic oscillators coupled to each other through

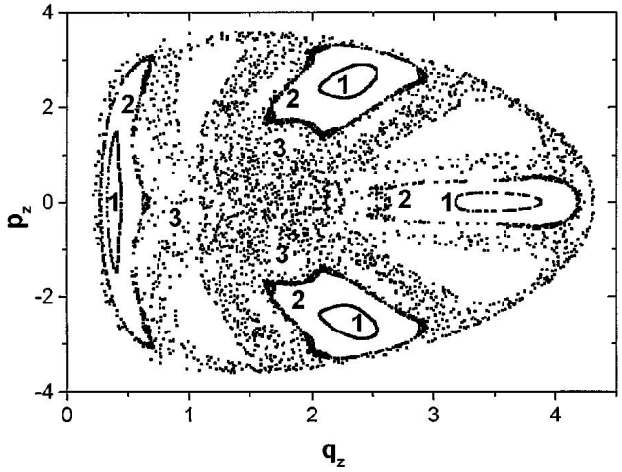

Figure 1: Poincare map for an abrupt change of the frequencies $\omega_{0i} \to \omega_{1i}$. The phase-space trajectories for the initial sets $\omega_{0i} = \{5.4, 5.4, 4.6\}$, $\omega_{0i} = \{6.6, 6.6, 4.2\}$, and $\omega_{0i} = \{6.5, 6.5, 4.2\}$ are labeled as 1, 2, and 3, respectively.

the non-linear term of volume scaling $\bar{\omega}_0^2/\mathcal{V}$. This Hamiltonian and scaling equations (11) are independent of the interaction between particles, although we are considering the Thomas-Fermi regime where the interaction is very important. This is a consequence of harmonicity of the trapping potential, which at the same time is a major reason for the existence of the scaling approach. One thus sees that the evolution of Thomas-Fermi condensates in the scaling approach is governed only by the time dependence of the trap frequencies $\omega_i(t)$.

Solutions of Eqs. (11) determine the evolution of phase $\Phi(\mathbf{r}, t)$ and the condensate density. For example, resonance frequencies of small shape oscillations of the condensate are the eigenfrequencies of small oscillations around the minimum value of the Hamiltonian (15) with $\omega_i(t) = \omega_{0i}$. This Hamiltonian is minimized at $q_i = \bar{\omega}_0/\omega_{0i}$, $p_i = 0$. In the vicinity of this point we arrive at the quadratic form which in the case of cylindrical symmetry gives the frequency of a quadrupole oscillation $\Omega_0 = \sqrt{2}\omega_{0r}$ (orbital angular momentum $M = 2$) and two frequencies of coupled monopole oscillations ($M = 0$):

$$\Omega_\pm = \omega_{0r}[9\beta^4 + 3\beta^2 \pm \sqrt{9\beta^4 - 16\beta 62 + 16})/2]^{1/2}; \tag{16}$$

where $\beta = \omega_{0z}/\omega_{0r}$ is the ratio of the axial to radial trap frequency. Resonance frequencies Ω_0 and Ω_- have been measured for Rb condensate in the JILA experiment [26] for $\beta = \sqrt{8}$ ($\Omega_- \approx 1.8\omega_{0r}$), and the frequencies $\Omega_\pm$ in the experiment at MIT [27] for $\beta = 0.08$ ($\Omega_+ \approx 2\omega_{0r}$, $\Omega_- \approx 1.58\omega_{0z}$).

The scaling equations (11) determine the character of the expansion of the condensate after the trap is abruptly switched off ($\omega_i = 0$ for $t \geq 0$). At times t greatly exceeding the lowest oscillation period the expansion becomes free in all directions and $\dot{b}_i = \text{const}$. A characteristic expansion velocity is governed by the velocity of sound in the initial condensate. However, due to anisotropy in the initial density gradient the velocity depends on the direction of expansion. In cylindrical traps the asymmetry of free expansion is characterized by the ratio of the axial to radial size, R_z/R_r. In the limiting case of $\beta \ll 1$, studied in the MIT experiment [28], the solution of scaling equations (11) gives $R_z/R_\rho = \pi\beta/2$ for $t \to \infty$. The expansion predominantly occurs in the radial direction, and the initially cigar-shaped condensate becomes pancake-shaped.

Collisionless thermal (non-condensed) gases expand symmetrically with thermal velocities $v_T \sim \sqrt{T/m}$ for any initial anisotropy of the trap. Therefore, observation of asymmetry in the expansion of dilute clouds in the first JILA [1] and MIT [2] experiments was the key evidence for BEC in the initial trapped cloud.

In spherical traps the solution of Eqs. (11) for a fast and strong change of the trap frequencies shows large undamped oscillations of the condensate density and phase. In anisotropic traps,

the coupling between different degrees of freedom through the non-linear term of volume scaling in the Hamiltonian H_{sd} can lead to stochastization of motion of the scaling parameters b_i [20]. Accordingly, the evolution of the condensate becomes stochastic. We will give an example where without changing the cylindrical symmetry the frequencies were abruptly changed from ω_{0i} to $\omega_{1i} = \{1.7, 1.7.1\}$. Fig.1 shows the Poincare map for three phase-space trajectories corresponding to three different sets of initial frequencies. The mapping points for the initial set $\omega_{0i} = \{5.4, 5.4, 6\}$ describe almost regular quasiperiodic motion in the vicinity of a second-order non-linear resonance. Points for $\omega_{0i} = \{6.6, 6.6, 4.2\}$ show that a large part of the phase space is occupied by stochastic motion. For the initial set $\omega_{0i} = \{6.5, 6.5, 4.2\}$ one finds an unstable trajectory intermediate between quasiperiodic motion and chaos.

Stochastic evolution of a condensate has been found in numerical calculations beyond the scaling approach [29, 31]. Various aspects of stochastization in the dynamics of trapped condensates have been discussed in literature (see, e.g., [30, 32]). In the cases 1 and 2 in Fig.1 the time dependence of the axial and radial sizes of the condensate is very irregular and can even "imitate" the relaxation behavior. It is important to emphasize that chaotic evolution of the condensate density and, especially, of the phase $\Phi(\mathbf{r}, t)$ makes the system vulnerable to the appearance of real relaxation and irreversibility under a small external influence.

3 Elementary excitations

Elementary excitations of a Bose-Einstein condensate, i.e. small oscillations around the equilibrium value of the condensate wave function ψ_0, represent a primary issue for understanding the macroscopic quantum behavior of the system. In particular, the character of the excitations determines the response of the system to external perturbations and is responsible for quantum depletion of the condensate. The presence of the trapping potential introduces a finite size of the system and provides a discrete structure of the excitation spectrum. In this section we discuss the Bogoliubov-de Gennes mean-field approach for finding the spectrum and wave functions of excitations of a trapped condensate.

We consider an equilibrium Bose-condensed gas in an external potential $V(\mathbf{r})$ (1) with constant frequencies ω_i. We then use the separation (4) of the field operator into the condensed and non-condensed parts and turn to the grand-canonical Hamiltonian $\hat{H}_\mu = \hat{H} - \mu\hat{\psi}^\dagger\hat{\psi}$, where $\hat{H}$ is given by Eq.(2). Assuming that the condensate density greatly exceeds the density of non-condensed particles we omit terms proportional to $\hat{\psi}^3$ and $\hat{\psi}^4$ in the grand-canonical Hamiltonian and write it as

$$\hat{H}_\mu = H_0 + \int d\mathbf{r}\Big\{\hat{\psi}'^\dagger\Big[-(\hbar^2/2m)\Delta + V(\mathbf{r}) - \mu + 2g|\psi_0|^2\Big]\hat{\psi}'\Big\} + (g/2)\Big[\psi_0^2\hat{\psi}'^\dagger\hat{\psi}'^\dagger + \psi_0^{*2}\psi'\psi'\Big], \tag{17}$$

where

$$H_0 = \int d\mathbf{r}\psi_0^*\left[-(\hbar^2/2m)\Delta + V(\mathbf{r}) - \mu + (g/2)|\psi_0|^2\right]\psi_0.$$

Owing to Eq.(7) the part of the Hamiltonian, which is linear in $\hat{\psi}'$, is equal to zero. The bilinear Hamiltonian $\hat{H}_\mu$ can be reduced to a diagonal form

$$\hat{H}_\mu = H_0 + \sum_\nu \varepsilon_\nu \hat{a}_\nu^\dagger \hat{a}_\nu \tag{18}$$

by using the Bogoliubov transformation generalized to the spatially inhomogeneous case [33]:

$$\psi'(\mathbf{r}, t) = \sum_\nu \Big[u_\nu \hat{a}_\nu(\mathbf{r})\mathrm{e}^{-i\varepsilon_\nu t} - v_\nu^*(\mathbf{r})\hat{a}_\nu^\dagger \mathrm{e}^{i\varepsilon_\nu)t}\Big]\,\mathrm{e}^{-i\mu t}$$

Here $\hat{a}_\nu$ and $\hat{a}_\nu^\dagger$ are (Schrödinger) annihilation and creation operators of an excitation characterized by a set of quantum numbers ν. The Hamiltonian $\hat{H}_\mu$ takes the form (18) if the functions u_ν, v_ν

satisfy the Bogoliubov-de Gennes equations

$$\left(-\frac{\hbar^2}{2m}\Delta+V(\mathbf{r})-\mu\right)u_\nu+g|\psi_0|^2(2u_\nu-v_\nu) \;=\; \varepsilon_\nu u_\nu, \tag{19}$$

$$\left(-\frac{\hbar^2}{2m}\Delta+V(\mathbf{r})-\mu\right)v_\nu+g|\psi_0|^2(2v_\nu-u_\nu) \;=\; -\varepsilon_\nu v_\nu. \tag{20}$$

The condensate wave function in Eqs. (19), (20) is taken to be real, and the functions u_ν, v_ν are normalized by the condition

$$\int d\mathbf{r}\,(u_\nu u^*_{\nu\prime} - v_\nu v^*_{\nu\prime}) = \delta_{\nu\nu\prime}.$$

Taking into account that ψ_0 obeys the Gross-Pitaevskii equation (7) we reduce Eqs. (19) and (20) to equations for the functions $f_{\nu\pm} = u_\nu \pm v_\nu$:

$$\frac{\hbar^2}{2m}\left(-\Delta+\frac{\Delta\psi_0}{\psi_0}\right)f_{\nu+} = \varepsilon_\nu f_{\nu-}, \tag{21}$$

$$\frac{\hbar^2}{2m}\left(-\Delta+\frac{\Delta\psi_0}{\psi_0}\right)f_{\nu-} + 2g|\psi_0|^2 f_{\nu-} = \varepsilon_\nu f_{\nu+}. \tag{22}$$

In the case of Thomas-Fermi condensates one has a small parameter

$$\zeta = \hbar\bar{\omega}/\mu \ll 1, \tag{23}$$

and the Bogoliubov-de Gennes equations for low-energy excitations ($\varepsilon_\nu \ll \mu$) are significantly simplified. The condition $\varepsilon_\nu \ll \mu$ corresponds to the hydrodynamic limit for the excitations. The functions $f_{\nu\pm}$ describe the phase and density fluctuations related to the excitation mode ν:

$$\hat{\phi}_\nu = (i/2\psi_0) f_{\nu+}\hat{a}_\nu \exp(-i\varepsilon_\nu t) + h.c., \tag{24}$$

$$\hat{\delta n} = \psi_0\, f_{\nu-}\hat{a}_\nu \exp(-i\varepsilon_\nu t) + h.c. \tag{25}$$

One then sees that Eqs. (21) and (22) are nothing else than the continuity and Euler equations. Inequality (23) allows one to omit the quantum pressure term, that is the first term in left-hand side of Eq.(22). This term scales as ζ^2/μ and is small compared to the second term in this equation, except near the border of the condensate spatial region. Then, turning to reduced coordinates $y_i = r_i/R_i$ we obtain $f_{\nu\pm} = [(2\mu(1-y^2)/\varepsilon_\nu)^{\pm 1/2} W_\nu$, where $y^2 = \sum_i y_i^2$ and the function W_ν satisfies the equation

$$\sum_i \omega_i^2 \left[(1-y^2)\frac{d^2}{dy_i^2} - 2y_i\frac{d}{dy_i}\right] W_\nu + 2\varepsilon_\nu^2 W_\nu = 0. \tag{26}$$

This approach has been first developed by Stringari [34] directly from the consideration of the density and phase fluctuations. Eq.(26) shows that the spectrum of low-energy excitations of Thomas-Fermi condensates is independent of the interaction between particles and is governed by the trap frequencies, which is a consequence of harmonicity in the trapping potential. In any other trapping field the dependence on the interaction will be pronounced.

In spherical traps one has a complete separation of variables and the excitations are charaterized by the orbital angular momentum l, its projection on the quantization axis m_l, and by the radial quantum number j which is a positive integer. We then have $W_\nu = w(y)Y_{lm_l}(\theta,\varphi)$ and Eq.(26) becomes a hypergeometrical differential equation for the function w:

$$x(1-x)\frac{d^2w}{dx^2} + \left[l+\frac{3}{2} - \left(l+\frac{5}{2}\right)x\right]\frac{dw}{dx} + \left(\frac{\varepsilon^2}{2} - \frac{l}{2}\right)w = 0,$$

where $x = y^2$. The solution of this equation, convergent at $x = 0$, is the hypergeometrical function that converges at the border of the condensate spatial region ($x = 1$) only when reduced to a polynomial. This immediately gives the excitation spectrum [34]

$$\varepsilon_{jl} = \hbar\omega(2j^2 + 2jl + 3j + l)^{1/2}, \tag{27}$$

and expresses the function w through classical Jacobi polynomials:

$$w_{jl} = [(4j + 2l + 3)/R^3]^{1/2} y^l P_j^{(l+1/2),0}(1 - 2y^2).$$

Due to the interaction between particles the low-energy excitations have collective character and the spectrum (27) is quite different from that for a collisionless thermal gas.

In cylindrical traps excitations are characterized by the projection of the orbital angular momentum on the cylinder axis, m, and their wave functions can be written as $W_\nu = y_\rho^{|m|} B_{jm} \exp im\varphi$, where B_{jm} is expressed in terms of polynomials of power j of the reduced radial (y_ρ) and axial (y_z) coordinates [35, 36]. The eigenstates are characterized by the axial parity and by the power of the polynomial. For a given m and odd j one has $(j + 1)/2$ excitation modes, and for an even j the number of modes is equal to $(j + 2)/2$. Actually, in eliptical coordinates one finds a complete separation of variables [36], which brings in a third quantum number for the eigenstates. A scheme for finding energies and wave functions of low-energy excitations in cylindrical traps has been described in Refs. [35, 36]. In particular, for quadrupole and monopole modes we arrive at the same eigenfrequencies as derived in the previous section from the scaling approach.

In non-symmetrical traps the functions W_ν are expressed in terms of polynomials of y_i and the eigenstates are characterized by a power of the polynomial [35, 37]. In this case one also finds a complete separation of variables [37].

A complete separation of variables in spherical traps is present at any excitation energy. This allows a straightforward numerical and, in certain limits, analytical solution of Eqs. (21), (22) at an arbitrary ε_ν [38, 39]. In cylindrical traps the situation is quite different as the problem is completely separable only for $\varepsilon_\nu \ll \mu$, or in the opposite limit $\varepsilon_\nu \gg \mu$ where the interaction between particles is not important. At intermediate energies $\varepsilon \sim \mu$ the spectrum becomes very irregular. For this case the study of classical dynamics of Bogoliubov-de Gennes quasiparticles shows stochastization of their motion. This allows the use of the statistical Wigner-Dyson approach [40, 41] for finding the distribution of energy levels at a given value of the projection of the angular momentum on the cylinder axis [13].

4 Critical temperature

Studies of a sharp cross-over to the BEC regime in trapped gases encounter a general problem related to the dependence of the critical temperature T_c on the interaction between particles. Actually, in trapped gases one has two reasons for this dependence. The first one is related to many-body effects beyond the mean-field theory, which are also present in the uniform case. Another reason is that the repulsive interaction between particles in a trap expands the gas cloud, with a consequent decrease of the density and critical temperature [6]. In the dilute limit, where $na^3 \ll 1$, both effects are expected to be small. Nevertheless, first measurements of T_c at JILA [16] indicate a negative shift of T_c by about 6% from the ideal gas value T_c^0.

We first discuss the interaction-induced shift of T_c in the uniform case. This problem has a long prehistory and most studies predict an increase of the critical temperature [42, 43, 44, 45, 46, 47, 48, 49, 50]. In the dilute limit the critical temperature rises linearly with the scattering length a. The relative shift of T_c is given by the relation

$$\frac{\delta T_c}{T_c} = C(na^3)^{1/2}, \tag{28}$$

where $C > 0$ is a dimensionless constant. However, there is a large discrepancy in the values of the constant C presented in literature. This is not surprising as one is dealing with the region of critical fluctuations, where perturbation theory breaks down and the physics that determines T_c is non-perturbative.

The problem of finding δT_c for a weakly interacting gas is related to solving static three-dimensional $|\psi|^4$ field theory [46]. The key point here is universality of the long-wave behavior of this theory in the fluctuation region at the transition point [48]. All such theories lead to a generic

long-wave Hamiltonian (see, e.g., [46])

$$\mathcal{H} = \int d\mathbf{r}\,\{(\hbar^2/2m)|\nabla\psi|^2 + (g/2)|\psi|^4\}. \tag{29}$$

From this universality one finds that the shift of the critical density, which is not sensitive to the ultraviolet cutoff of the theory, follows from the equation

$$\delta n_c(T) = -Dm^3T^2g/\hbar^6, \tag{30}$$

where D is a universal constant. Then, the shift of the critical temperature, which is sensitive to short-wave physics, can be obtained for a particular system from the relation

$$\frac{\delta T_c}{\delta n_c} = -\frac{dT_c^0(n)}{dn}. \tag{31}$$

For an ideal gas the critical temperature $T_c = 3.31\hbar^2n^{2/3}/m$ and we immediately arrive at Eq.(28). The positive sign of the constant C can be established from the change in the energy of low momentum particles near T_c [44].

The first numerical calculation of the shift δT_c was an *ab initio* simulation using a path-integral Monte Carlo method [43]. The results of this approach are consistent with Eq.(28). An alternative Monte Carlo approach [45] was based on an assumption that Eq.(28) can be obtained in a sophisticated perturbative way. However, these two calculations arrived at very different values of C. A reliable value of this constant, namely $C \approx 1.3$, has been obtained in recent lattice Monte Carlo studies of the $|\psi|^4$ model [48, 49].

Theoretical derivations of the shift δT_c are in a resonably good agreement with the results of Refs. [48, 49]. On the basis of the $|\psi^4|$ model, self-consistent calculation of the quasiparticle spectrum at low momenta at the transition, give $C \approx 2.9$. Calculations using general renormalization group arguments [47] lead to $C \approx 2.3$ (see also [51]). The recent contributions [52, 53] find a nonanalytical correction $\propto a^2 \ln a$ to the previously calculated [46, 47] shift of the critical temperature (see also [42]). This correction does not introduce a new length scale beyond $n^{-1/3}$. It is negative and, because of its logarithmic character, leads to a strong dependence on a even in the very dilute limit. The presence of this nonanalytical correction, to a certain extent explains the discrepancy between theoretical derivations [46, 47] and Monte Carlo calculations [48, 49].

In a trapped gas the cross-over temperature T_c is well defined for a very large number of particles N. As already mentioned, in this case one has another contribution to the shift of T_c, originating from the dependence of the density profile of the gas on the interaction between particles. In particular, the interparticle repulsion decreases the central density and leads to a negative shift [6]

$$\frac{\delta T_c}{T_c^0} = -1.3\frac{a}{l_0}N^{1/6}, \tag{32}$$

where l_0 is the harmonic oscillator length of the trap. Note that the quantity $(a/l_0)N^{1/6}$ is of the order of $n_{\max}^{1/3}$, with $n_{\max}$ being the central density of the cloud. Therefore, the shift (32) has the same scaling as the non-perturbative shift (28) discussed above for the uniform case. More detailed discussions of the shift of the critical temperature in a trapped gas one finds in Refs. [54, 55].

5 Phase coherence

Phase coherence properties of Bose-condensed gases attract a great deal of interest as they provide deeper understanding of the nature of BEC states. The first phase coherence experiments relied on the interference of two independently prepared condensates [7] and on the measurement of the phase coherence length and/or single-particle correlations [56, 57, 58]. These experiments showed that trapped condensates are phase coherent, in accordance with a common understanding of BEC in 3D gases. In equilibrium, the fluctuations of density and phase are important only in a narrow temperature range near T_c and are suppressed outside this region.

In this section we show that the phase coherence properties of three-dimensional (3D) Thomas-Fermi condensates depend on the geometry of the system [17]. In particular, strong elongation of the gas in one direction brings in the interesting physics of one-dimensional (1D) systems. In very elongated 3D condensates, the axial phase fluctuations manifest themselves even at temperatures far below T_c. Then, as the density fluctuations are suppressed, the equilibrium state will be a *condensate with fluctuating phase* (quasicondensate) similar to that in 1D trapped gases [59]. Decreasing T below a sufficiently low temperature, the 3D quasicondensate gradually transforms into a true condensate.

We consider a 3D Bose gas in an elongated cylindrical harmonic trap and analyze the behavior of the single-particle correlation function. The natural assumption of the existence of a true condensate at $T = 0$ automatically comes out of these calculations. In the Thomas-Fermi regime, where the repulsive interparticle interaction greatly exceeds the radial (ω_ρ) and axial (ω_z) trap frequencies, the density profile of the zero-temperature condensate has the well-known shape $n_0(\rho, z) = n_{0m}(1 - \rho^2/R^2 - z^2/L^2)$, where $n_{0m} = \mu/g$ is the maximum condensate density. Under the condition $\omega_\rho \gg \omega_z$, the radial size of the condensate, $R = (2\mu/m\omega_\rho^2)^{1/2}$, is much smaller than the axial size $L = (2\mu/m\omega_z^2)^{1/2}$.

Fluctuations of the density of the condensate are dominated by the excitations with energies of the order of μ. The wavelength of these excitations is much smaller than the radial size of the condensate. Hence, the density fluctuations have the ordinary 3D character and are small. Therefore, one can write the total field operator of atoms as

$$\hat{\psi}(\mathbf{r}) = \sqrt{n_0(\mathbf{r})}\exp(i\hat{\phi}(\mathbf{r})), \tag{33}$$

where the operator of the phase is

$$\hat{\phi}(\mathbf{r}) = \sum_\nu \hat{\phi}_\nu(\mathbf{r}), \tag{34}$$

and the operator $\phi_\nu(\mathbf{r})$ is given by Eq.(24). The single-particle correlation function is then expressed through the mean square fluctuations of the phase (see, e.g. [60]):

$$\langle\hat{\psi}^\dagger(\mathbf{r})\hat{\psi}(\mathbf{r}')\rangle = \sqrt{n_0(\mathbf{r})n_0(\mathbf{r}')}\exp\{-\langle[\delta\hat{\phi}(\mathbf{r},\mathbf{r}')]^2\rangle/2\}, \tag{35}$$

with $\delta\hat{\phi}(\mathbf{r}, \mathbf{r}') = \hat{\phi}(\mathbf{r}) - \hat{\phi}(\mathbf{r}')$.

The excitations of elongated condensates can be divided into two groups: "low energy" axial excitations with energies $\epsilon_\nu < \hbar\omega_\rho$, and "high energy" excitations with $\epsilon_\nu > \hbar\omega_\rho$. The latter have 3D character as their wavelengths are smaller than the radial size R. Therefore, as in ordinary 3D condensates, these excitations can only provide small phase fluctuations. The "low-energy" axial excitations have wavelengths larger than R and exhibit a pronounced 1D behavior. These excitations give the most important contribution to the long-wave axial fluctuations of the phase.

The solution of the Bogolyubov-de Gennes equations (21), (22) for the low-energy axial modes gives the spectrum $\varepsilon_j = \hbar\omega_z\sqrt{j(j+3)/4}$ [61], where j is a positive integer. The wavefunctions f_j^+ of these modes have the form

$$f_j^+(\mathbf{r}) = \sqrt{\frac{(j+2)(2j+3)gn_0(\mathbf{r})}{4\pi(j+1)R^2L\varepsilon_j}}P_j^{(1,1)}\left(\frac{z}{L}\right), \tag{36}$$

where $P_j^{(1,1)}$ are Jacobi polynomials. Note that the contribution of the low-energy axial excitations to the phase operator (34) is independent of the radial coordinate ρ.

Relying on Eqs. (24), (34) and (36), we now calculate the mean square axial fluctuations of the phase at distances $|z - z'| \ll R$. As in 1D trapped gases [59], the vacuum fluctuations are small for any realistic axial size L. The thermal fluctuations are determined by the equation

$$\langle[\delta\hat{\phi}(z,z')]^2\rangle_T = \sum_{j=1}^{\infty}\frac{\pi\mu(j+2)(2j+3)}{15(j+1)\varepsilon_j N_0}\times$$
$$\left(P_j^{(1,1)}\left(\frac{z}{L}\right) - P_j^{(1,1)}\left(\frac{z'}{L}\right)\right)^2 N_j, \tag{37}$$

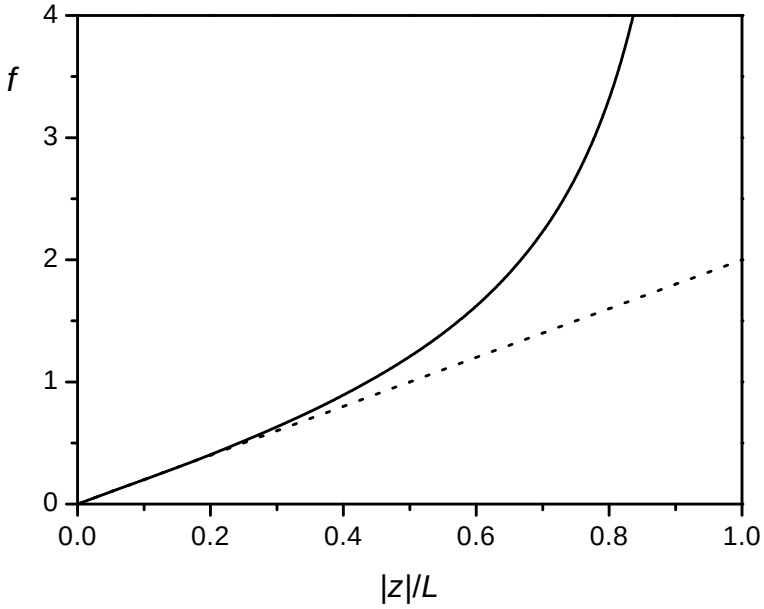

Figure 2: The function $f(z/L)$. The solid curve shows the numerical result, and the dotted line is $f(z) = 2|z|/L$ following from Eq.(38).

with $N_0 = (8\pi/15)n_{0m}R^2L$ being the number of Bose-condensed particles, and N_j the equilibrium occupation numbers for the excitations. Strictly speaking, to zero order in perturbation theory one should make the summation in Eq.(37) only over excitations with energies $\varepsilon_j < \mu$. This is, however, not a problem as the main contribution to the sum over j comes from several lowest excitation modes. At temperatures $T \gg \hbar\omega_z$ we may put $N_j = T/\varepsilon_j$, and in the central part of the cloud ($|z|, |z'| \ll L$) a straightforward calculation yields

$$\langle[\delta\hat{\phi}(z,z')]^2\rangle_T = \delta_L^2|z-z'|/L, \tag{38}$$

where the quantity δ_L^2 represents the phase fluctuations on a distance scale $|z - z'| \sim L$ and is given by

$$\delta_L^2(T) = 32\mu T/15N_0(\hbar\omega_z)^2. \tag{39}$$

Note that at any z and z' the ratio of the phase correlator (37) to δ_L^2 is a universal function of z/L and z'/L:

$$\langle[\delta\hat{\phi}(z,z')]^2\rangle_T = \delta_L^2(T)f(z/L, z'/L). \tag{40}$$

In Fig.2 we present the function $f(z/L) \equiv f(z/L, -z/L)$ calculated numerically from Eq.(37).

The phase fluctuations decrease with temperature. As the chemical potential is $\mu = (15N_0g/\pi)^{2/5}(m\bar{\omega}^2/8)^{3/5}$ ($\bar{\omega} = \omega_\rho^{2/3}\omega_z^{1/3}$), Eq.(39) can be rewritten in the form

$$\delta_L^2 = (T/T_c)(N/N_0)^{3/5}\delta_c^2. \tag{41}$$

The presence of the 3D BEC transition in elongated traps requires the inequality $T_c \gg \hbar\omega_\rho$ and, hence, limits the aspect ratio to $\omega_\rho/\omega_z \ll N$. The parameter δ_c^2 is given by

$$\delta_c^2 = \frac{32\mu(N_0 = N)}{15N^{2/3}\hbar\bar{\omega}}\left(\frac{\omega_\rho}{\omega_z}\right)^{4/3} \propto \frac{a^{2/5}m^{1/5}\omega_\rho^{22/15}}{N^{4/15}\omega_z^{19/15}}. \tag{42}$$

Except for a narrow interval of temperatures just below T_c, the fraction of non-condensed atoms is small and Eq.(41) reduces to $\delta_L^2 = (T/T_c)\delta_c^2$. Thus, the phase fluctuations can be important at large values of the parameter δ_c^2, whereas for $\delta_c^2 \ll 1$ they are small on any distance scale and one has a true Bose-Einstein condensate.

The single-particle correlation function is determined by Eq.(35) only if the condensate density n_0 is much larger than the density of non-condensed atoms, n'. Otherwise, this equation should be completed by terms describing correlations in the thermal cloud. For T close to T_c and $N_0 \ll N$, assuming $n' \ll n_0$ the density fluctuations are still suppressed, and Eq.(41) gives $\delta_L^2 = (N/N_0)^{3/5}$.

We will focus our attention on the case where $N_0 \approx N$ and the presence of the axial phase fluctuations is governed by the parameter δ_c^2. For $\delta_c^2 \gg 1$, the nature of the Bose-condensed state depends on temperature. In this case we can introduce a characteristic temperature

$$T_\phi = 15(\hbar\omega_z)^2 N/32\mu \tag{43}$$

at which the quantity $\delta_L^2 \approx 1$ (for $N_0 \approx N$). In the temperature interval $T_\phi < T < T_c$, the phase fluctuates on a distance scale smaller than L. Thus, as the density fluctuations are suppressed, the Bose-condensed state is a condensate with fluctuating phase or quasicondensate. The expression for the radius of phase fluctuations (phase coherence length) follows from Eq.(38) and is given by

$$l_\phi \approx L(T_\phi/T). \tag{44}$$

The phase coherence length l_ϕ greatly exceeds the correlation length $l_c = \hbar/\sqrt{m\mu}$. Eqs. (44) and (43) give the ratio $l_\phi/l_c \approx (T_c/T)(T_c/\hbar\omega_\rho)^2 \gg 1$. Therefore, the quasicondensate has the same density profile and local correlation properties as the true condensate. However, the phase coherence properties of quasicondensates are drastically different.

The decrease of temperature to well below T_ϕ makes the phase fluctuations small ($\delta_L^2 \ll 1$) and continuously transforms the quasicondensate into a true condensate. There is no sharp cross-over.

Most important is the dependence of δ_c^2 on the aspect ratio of the cloud ω_ρ/ω_z, whereas the dependence on the number of atoms and on the scattering length is comparatively weak. Fig.3 shows $T_c/T_\phi = \delta_c^2$, μ/T_ϕ, and the temperature T_ϕ as functions of ω_ρ/ω_z for rubidium condensates at $N = 10^5$ and $\omega_\rho = 500$ Hz. From these results we see that 3D quasicondensates can be obtained in elongated geometries with $\omega_\rho/\omega_z \gtrsim 50$.

The phase fluctuations are very sensitive to temperature. From Fig.3 we see that one can have $T_\phi/T_c < 0.1$, and the phase fluctuations are still significant at $T < \mu$, where only a tiny indiscernible thermal cloud is present.

This suggests a principle for thermometry of 3D Bose-condensed gases with indiscernible thermal clouds. If the sample is not an elongated quasicondensate by itself, it is first transformed to this state by adiabatically increasing the aspect ratio ω_ρ/ω_z. This does not change the ratio T/T_c as long as the condensate remains in the 3D Thomas-Fermi regime. Second, the phase coherence length l_ϕ or the single-particle correlation function are measured. These quantities depend on temperature if the latter is of the order of T_ϕ or larger. One thus can measure the ratio T/T_c for the initial cloud, which is as small as the ratio T_ϕ/T_c for the elongated cloud.

One can measure the phase fluctuations and distinguish between quasicondensates and true BEC's in various types of experiments. In a gedanken "juggling" experiment described in [59] one can directly measure the single-particle correlation function. The latter is obtained by repeatedly ejecting small clouds of atoms from the parts z and z' of the sample and averaging the pattern of interference between them in the detection region over a large set of measurements. As follows from Eqs. (39) and (40), for $z' = -z$ the correlation function depends on temperature as $\exp\{-\delta_L^2(T) f(z/L)/2\}$, where $f(z/L)$ is given in Fig.2.

Pronounced phase fluctuations have been first observed in Hannover experiments with very elongated cylindrical 3D condensates of up to 10^5 rubidium atoms [18]. The expanding cloud released from the trap was imaged after 25 ms of time of flight and the images showed clear modulations of the density (stripes) in the axial direction (see Fig.4). The physical reason for the appearance of stripes is the following. In a trap the density distribution does not feel the presence of the phase fluctuations, since the mean-field interparticle interaction prevents the transformation of local velocity fields provided by the phase fluctuations into modulations of the density. After switching off the trap, the cloud rapidly expands in the radial direction, whereas the axial phase fluctuations remain unaffected. As the mean-field interaction drops to almost zero, the axial velocity fields are then converted into the density distribution.

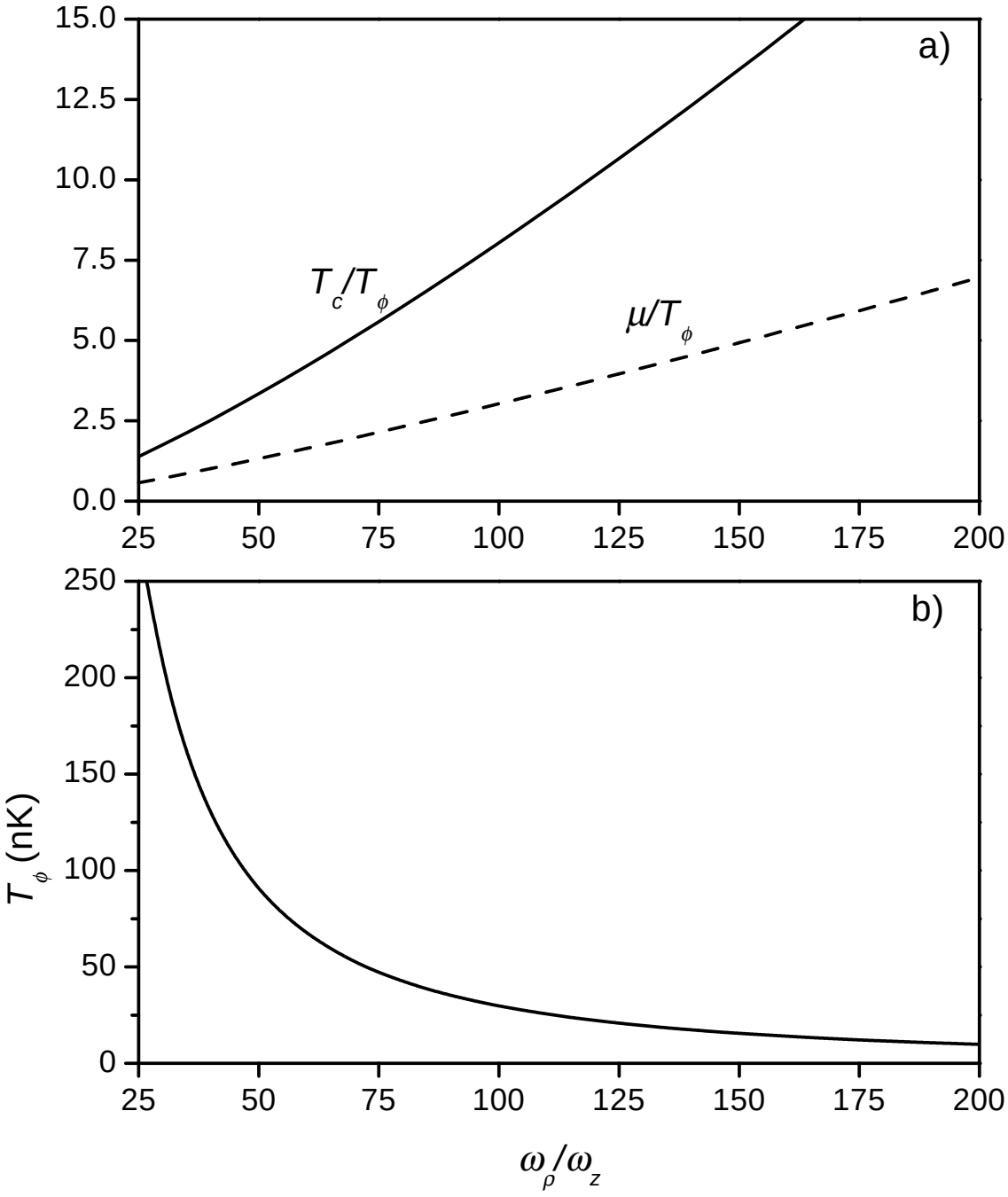

Figure 3: The ratios $T_c/T_\phi = \delta_c^2$ and μ/T_ϕ in (a) and the temperature T_ϕ in (b), versus the aspect ratio ω_ρ/ω_z for trapped Rb condensates with $N = 10^5$ and $\omega_\rho = 500$ Hz.

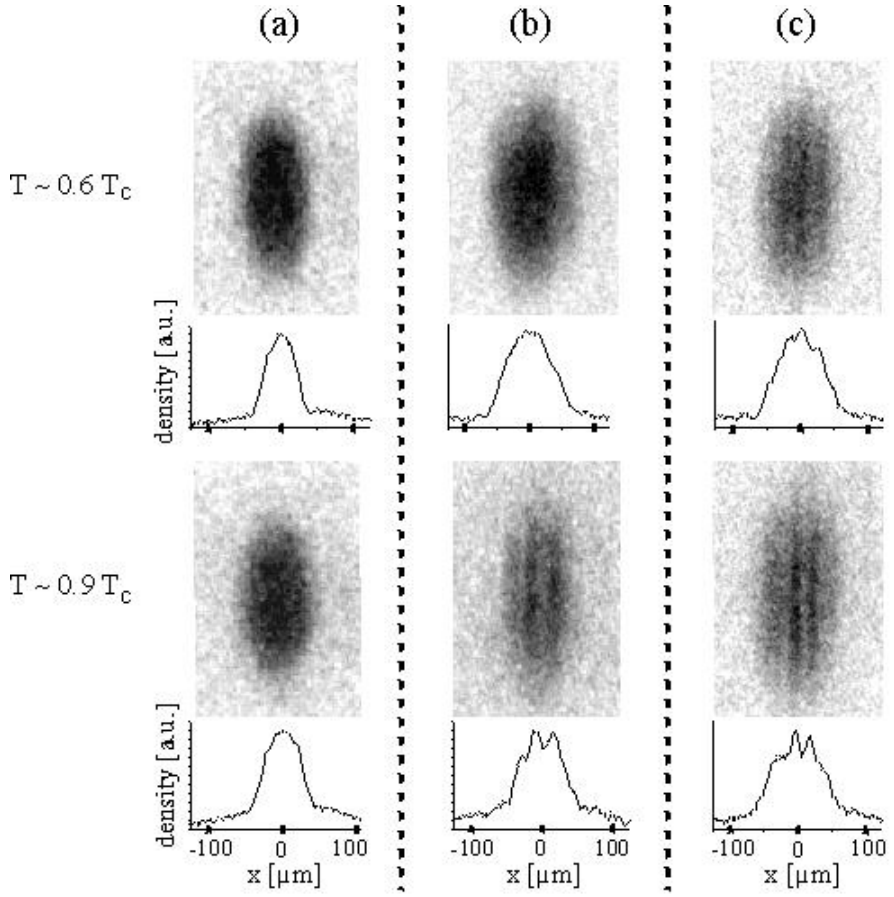

Figure 4: Absorption images and corresponding density profiles of BECs after 25 ms time-of-flight in the Hannover experiment for aspect ratios [$\omega_\rho/\omega_z = 10$ (a), 26 (b), 51 (c)].

The mean square modulations of the density in the expanding cloud provide a measure of the phase fluctuations in the initial trapped condensate. A direct relation between these quantities has been established from analytical and numerical solutions of the Gross-Pitaevskii equation for the expanding cloud, with explicitly included initial fluctuations of the phase [18]. The obtained phase coherence length was inversly proportional to T, in agreement with theory, and for most measurements it was smaller than the axial size L of the trapped Thomas-Fermi cloud. This implies that the measurements were performed in the regime of quasicondensation.

The properties of quasicondensates and the phase coherence length were measured directly in Bragg spectroscopy experiments with elongated rubidium BECs at Orsay [19]. In this type of experiment one measures the momentum distribution of particles in the trapped gas. The use of axially counter-propagating laser beams to absorb a photon from one beam and emit it into the other one, results in axial momentum transfer to the atoms which have momenta at Doppler shifted resonance with the beams. These atoms form a small cloud which will axially separate from the rest of the sample provided the mean free path greatly exceeds the axial size L. The latter condition is assured at Orsay by applying the Bragg excitation after abruptly switching off the radial confinement of the trap. To build the momentum distribution one measures the fraction of diffracted atoms versus the detuning between the counterpropagating beams.

The Orsay experiment [19] finds a Lorentzian momentum distribution characteristic of quasicondensates with axially fluctuating phase [62], whereas a true condensate has a Gaussian distribution. The width of the Lorentzian momentum distribution is related to the phase coherence length at the trap center as $\Delta p_\phi \approx 0.67\hbar/l_\phi$. Therefore, the width of the Bragg spectrum is

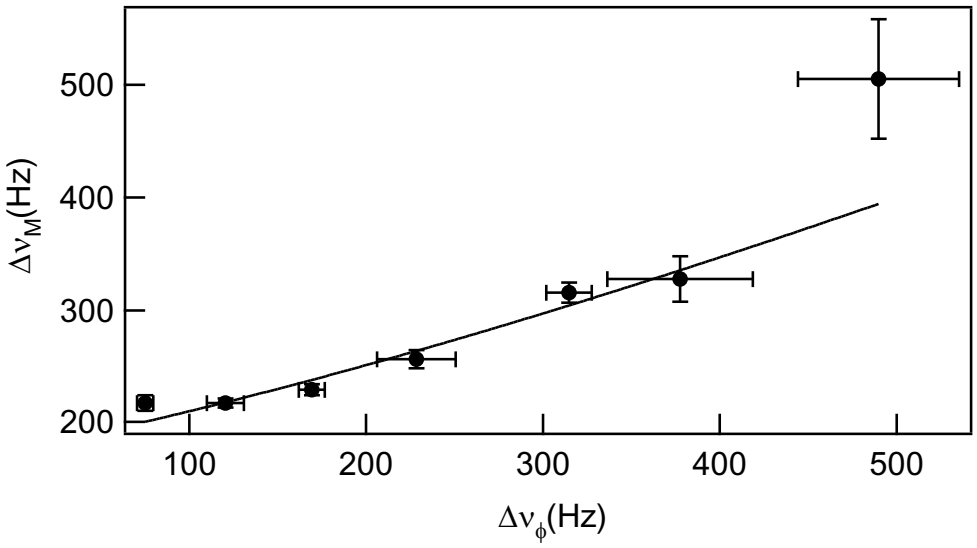

Figure 5: Half-width $\Delta\nu_M$ of the Bragg spectrum versus the parameter $\Delta_\phi \propto 1/l_\phi$ (see text) in the Orsay experiment. The solid line is a fit assuming a Voigt profile for the spectrum.

$\Delta\nu_M \approx 0.67\Delta\nu_\phi$, where $\Delta\nu_\phi = \hbar k_L/\pi m l_\phi$, and k_L is the photon momentum. According to the theoretical analysis, the quantity $\Delta\nu_\phi$ should be proportional to the temperature. Fig.5 shows the measured spectral width Δ_M versus Δ_ϕ calculated by using l_ϕ following from theoretical approaches of Refs. [17, 62]. The coherence length deduced from the measurements of $\Delta\nu_M$ was in perfect agreement with theory. It was ranging from $L/6$ to $L/36$, which shows a deep penetration into the quasicondensate regime. The suppression of the density fluctuations was established through the measurement of the axial size of the cloud.

We believe that the studies of phase coherence in elongated condensates will reveal many new interesting phenomena. The measurement of phase correlators will allow one to study the evolution of phase coherence in the course of the formation of a condensate out of a non-equilibrium thermal cloud. This problem has a rich physics. For example, recent experiments on the formation kinetics of trapped condensates [63] indicate the appearance of non-equilibrium quasicondensates slowly evolving towards the equilibrium state.

6 Concluding remarks

We see that the use of condensed matter approaches for dilute quantum gases provides us with remarkable physics closely related to ongoing experiments. In the near future, even more exciting developments are expected, in particular in new directions of cold atom physics. We mention a novel system of strongly correlated atoms in an optical lattice, where the Mott-insulator-Superfluid transition has been recently observed for bosons [64]. Studies of this system have strong ties to both condensed matter physics and quantum computing. Another hot topic is related to ultracold trapped Fermi gases which recently have been cooled to quantum degeneracy [65]. A search for superfluidity in this system requires advanced theoretical approaches for describing strong-coupling regimes. The progress in atom chip technologies and optical techniques provides unique possibilities for creating 1D atomic systems, and exploration of their physics requires the development of exactly solvable models of theoretical physics.

References

[1] M.H. Anderson *et al.*, *Science* **269**, 198 (1995).

[2] K.B. Davis *et al.*, *Phys. Rev. Lett.* **75**, 3969 (1995).

[3] C.C. Bradley *et al.*, *Phys. Rev. Lett.* **75**, 1687 (1995).

[4] See for review W. Ketterle and N.J. van Druten, in: Advances in Atomic, Molecular and Optical Physics, B. Bederson and H. Walther (Ed.), Vol.37, p.181 (1996); J.T.M. Walraven, in: Quantum Dynamics of Simple Systems, G.-L. Oppo (Ed.), vol.44, p.315 (1994).

[5] See for review C. Cohen-Tannoudji in: Atomic Physics XIV, C.E. Wieman, D.J. Wineland and S.J. Smith (Ed.), AIP, New York, p.193 (1995); W.D. Phillips, *ibid*, p.211 (1995).

[6] F. Dalfovo *et al*, *Rev. Mod. Phys.* **71**, 463 (1999).

[7] M.R. Andrews *et al*, *Science* **275**, 637 (1997).

[8] E.A. Burt *et al*, *Phys. Rev. Lett.* **79**, 337 (1997).

[9] A.L. Fetter and A.A. Svidzinsky, *J. Phys. - Condensed Matter* **13**, R135 (2001).

[10] Yu.S Kivshar and G.P. Aqrawal, *Optical solitons: From fibers to photonic crystals*, Chapter 14 (Elsevier Science, USA, 2003).

[11] O.M. Marago *et al*, Phys. Rev. Lett. **85**, 692 (2000).

[12] C. Raman *et al*, *Phys. Rev. Lett.* **83**, 2502 (1999).

[13] P.O. Fedichev, G.V. Shlyapnikov, and J.T.M. Walraven, *Phys. Rev. Lett.* **80**, 2269 (1998); P.O. Fedichev and G.V. Shlyapnikov, *Phys. Rev. A* **58**, 3146 (1998) and references therein.

[14] B. Jackson and E. Zaremba, *Phys. Rev. Lett.* **88**, 033606 (2002); *ibid* **89**, 150402 (2002) and references therein.

[15] A.E. Muryshev *et al*, *Phys. Rev. Lett.* **89**, 110401 (2002).

[16] J.R. Ensher *et al*, *Phys. Rev. Lett.* **75**, 4984 (1996).

[17] D.S. Petrov, G.V. Shlyapnikov, and J.T.M. Walraven, *Phys. Rev. Lett.* **87**, 050404 (2001).

[18] S. Dettmer *et al*, *Phys. Rev. Lett.* **87**, 160406 (2001).

[19] S. Richard *et al*, cond-mat/0303137.

[20] Yu. Kagan, E.L. Surkov, and G.V. Shlyapnikov, *Phys. Rev. A* **54**, R1753 (1996); *ibid* **55**, R18 (1997).

[21] Y. Castin and R. Dum, *Phys. Rev. Lett.* **77**, 5315 (1996).

[22] L.P. Pitaevskii and A. Rosch, *Phys. Rev. A* **55**, R853 (1996).

[23] E.M. Lifshitz and L.P. Pitaevskii, *Statistical Physics, Part 2* (Pergamon Press, Oxford, 1980).

[24] V.V. Goldman, I.F. Silvera, and A. Leggett, *Phys. Rev. B* **24**, 2870 (1981).

[25] D.A. Huse and E.D. Siggia, *J. Low Temp. Phys.* **46**, 137 (1982).

[26] D.S. Jin *et al*, *Phys. Rev. Lett.* **77**, 420 (1996).

[27] M.-O. Mewes *et al*, *Phys. Rev. Lett.* **77**, 988 (1996).

[28] M.-O. Mewes *et al*, *Phys. Rev. Lett.* **77**, 416 (1996).

[29] A. Smerzi and S. Fantoni, *Phys. Rev. Lett.* **78**, 3589 (1997).

[30] F. Dalfovo *et al*, *Phys. Lett. A* **227**, 259 (1997).

[31] A. Sinatra *et al*, *Phys. Rev. Lett.* **82**, 251 (1999).

[32] M. Fliesser and R. Graham, *Physica D* **131**, 141 (1999) and references therein.

[33] P.G. de Gennes *Superconductivity of Metals and Alloys* (Benjamin, New York, 1966).

[34] S. Stringari, *Phys. Rev. Lett.* **77**, 2360 (1996).

[35] P. Ohberg *et al*, *Phys. Rev. A* **56**, R3346 (1997).

[36] M. Fliesser *et al*, *Phys. Rev. A* **56**, R2533 (1997); ibid **56**, 4879 (1997).

[37] A. Csordas and R. Graham, *Phys. Rev. A* **59**, 1477 (1999).

[38] A. Csordas, R. Graham, and P. Szepfalusy, *Phys. Rev. A* **56**, 5179 (1997); *ibid* **57**, 4669 (1998).

[39] M. Guilleumas and L.P. Pitaevskii, *Phys. Rev. A* **61**, 013602 (1999).

[40] E.P. Wigner, *Math. Ann.* **53**, 36 (1951); *ibid* **62**, 548 (1955).

[41] F.J. Dyson, *J. Math. Phys.* **3**, 140 (1955).

[42] H.T.C. Stoof, *Phys. Rev. A* **45**, 8398 (1992); M. Bijlsma and H.T.C. Stoof, *Phys. Rev. A* **54**, 5085 (1996).

[43] P. Gruter, D. Ceperley, and F. Laloe, *Phys. Rev. Lett.* **79**, 3549 (1997).

[44] M. Holzmann, P. Gruter, and F. Laloe, *Eur. Phys. J. B* **10**, 739 (1999).

[45] M. Holzmann and W. Krauth, *Phys. Rev. Lett.* **83**, 2687 (1999).

[46] G. Baym *et al*, *Phys. Rev. Lett.* **83**, 1703 (1999).

[47] G. Baym, J.-P. Blaizot, and J. Zinn-Justin, *Europhys. Lett.* **49**, 150 (2000).

[48] V.A. Kashurnikov, N.V. Prokof'ev, and B.V. Svistunov, *Phys. Rev. Lett.* **87**, 120402 (2001).

[49] P. Arnold and G. Moore, *Phys. Rev. Lett.* **87**, 120401 (2001).

[50] See for review: G. Baym *et al*, *Eur. Phys. J. B* **24**, 104 (2001).

[51] P. Arnold and B. Tomasik, *Phys. Rev. A* **62**, 063604 (2000).

[52] M. Holzmann *et al*, *Phys. Rev. Lett.* **87**, 120403 (2001).

[53] P. Arnold, G. Moore, and B. Tomasik, *Phys. Rev. A* **65**, 013606 (2002).

[54] M. Houbiers, H.T.C. Stoof, and E.A. Cornell, *Phys. Rev. A* **56**, 2041 (1997).

[55] P. Arnold and B. Tomasik, *Phys. Rev. A* **64**, 053609 (2001).

[56] J. Stenger *et al.*, *Phys. Rev. Lett.* **80**, 4569 (1999).

[57] E.W. Hagley *et al*, *Science* **283**, 1706 (1999).

[58] I. Bloch *et al*, *Nature (London)* **403**, 166 (2000).

[59] D.S. Petrov, G.V. Shlyapnikov, and J.T.M. Walraven, *Phys. Rev. Lett.* **85**, 3745 (2000).

[60] V.N. Popov, *Functional Integrals in Quantum Field Theory and Statistical Physics*, (D. Reidel Pub., Dordrecht, 1983).

[61] S. Stringari, *Phys. Rev. A* **58**, 2385 (1998).

[62] F. Gerbier *et al*, cond-mat/0211094.

[63] I. Shvarchuk *et al*, *Phys. Rev. Lett.* **89**, 270404 (2002).

[64] M. Greiner *et al*, *Nature (London)* **415**, 39 (2002).

[65] B. De Marco and D.S. Jin, *Science* **285**, 1703 (1999); F. Schreck *et al*, *Phys. Rev. Lett.* **87**, 080403 (2001); A.G. Truscott *et al*, *Science* **291**, 2570 (2001); S.R. Granade *et al*, *Phys. Rev. Lett.* **88**, 120405 (2002); Z. Hadzibabic *et al*, *Phys. Rev. Lett.* **88**, 160401 (2002); G. Roatti *et al*, *Phys. Rev. Lett.* **89**, 150403 (2002); K.M. O'Hara *et al*, *Science* **298**, 2179 (2002).

G.V. Shlyapnikov
FOM Institute for Atomic and Molecular Physics,
Kruislaan 407
1098 SJ Amsterdam
The Netherlands